

## ORIGINAL ARTICLE

Iran J Allergy Asthma Immunol

August 2020; 19(4):397-408.

Doi: 10.18502/ijaai.v19i4.4114

# Leucine-rich Repeats and Immunoglobulin 1 (LRIG1) Ameliorates Liver Fibrosis and Hepatic Stellate Cell Activation via Inhibiting Sphingosine Kinase 1 (SphK1)/Sphingosine-1-Phosphate (S1P) Pathway

Wei Zhan<sup>1</sup>, Xin Liao<sup>2</sup>, Zhongsheng Chen<sup>3</sup>, Lianghe Li<sup>3</sup>, Tian Tian<sup>3,4</sup>, and Rui Li<sup>5</sup>

<sup>1</sup> Department of Colorectal Surgery, Affiliated Hospital of Guizhou Medical University, Guiyang, China

<sup>2</sup> Department of Imaging, Affiliated Hospital of Guizhou Medical University, Guiyang, China

<sup>3</sup> Guizhou Medical University, Guiyang, China

<sup>4</sup> Department of Pathology, Guiyang Maternal and Child Health Hospital, Guiyang, China

<sup>5</sup> Department of Traditional Chinese Medicine, Guizhou Provincial People's Hospital, Guiyang, China

Received: 24 June 2019; Received in revised form: 1 March 2020; Accepted: 10 March 2020

## ABSTRACT

To detect the leucine-rich repeats and immunoglobulin 1 (LRIG1) ameliorated liver fibrosis and hepatic stellate cell (HSC) activation via inhibiting sphingosine kinase 1 (SphK1)/Sphingosine-1-Phosphate (S1P) pathway.

C57BL/6 male mice (eight weeks old) were intraperitoneal injection with 10% carbon tetrachloride (CCl<sub>4</sub>) as an *in vivo* model. The LX-2 cells were induced as a model for *in vitro* study by TGF- $\beta$  (10 ng/mL).

The Hematoxylin-eosin (HE) staining, Masson staining, and Sirius red staining results showed that CCl<sub>4</sub> caused serious fibrosis and injury in liver tissue, high expression of type I collagen  $\alpha$ 1 chain (Col1 $\alpha$ 1) and  $\alpha$ -smooth muscle actin ( $\alpha$ -SMA) in liver tissue, while the LRIG1 expression level was significantly decreased in LX-2 cell lines. The LRIG1 ameliorated CCl<sub>4</sub>-induced liver fibrosis, indicated by the fibronectin,  $\alpha$ -SMA, LRIG1, SphK1, Col1 $\alpha$ 1, fibrin Connexin 1 (Fn1), tissue inhibitor of metalloproteinase-1 (TIMP1), sphingosine-1-phosphate (S1P), transforming growth factor-beta 1 (TGF- $\beta$ 1) expression level changes. Similar results were observed in TGF- $\beta$ 1 treated of LX-2 cells. However, the effects were attenuated by treatment with LRIG1. Moreover, SphK1 inhibitors abrogated the effect of LRIG1 on fibrosis.

These results demonstrated that LRIG1 improved liver fibrosis *in vitro* and *in vivo* via suppressing the SphK1/S1P pathway, indicating its potential use in the treatment of liver fibrosis.

**Keywords:** Carbon tetrachloride; Immunoglobulins; Leucine-rich repeats; Liver fibrosis; Sphingosine kinase; Sphingosine-1-phosphate

**Corresponding Author:** Rui Li, MD;

Department of Traditional Chinese Medicine, Guizhou Provincial People's Hospital, Zhongshan East Road 83, Guiyang, China.  
Tel: (+86 851) 8593 7011, E-mail: RuiLidfg@163.com

## INTRODUCTION

The chronic liver injury which is characterized by disruption of liver structure and excessive accumulation

of abnormal extracellular matrix (ECM) leads to liver fibrosis.<sup>1,2</sup> ECM transforms from collagen-rich IV/VI array to I/III-rich collagen during liver fibrosis, resulting in deformation of the liver's stiffness and sinusoidal structure.<sup>3</sup> Long-term liver fibrosis causes subsequent liver dysfunction and cirrhosis, even liver cancer.<sup>4</sup> Stimulation of hepatic stellate cells (HSC) is characterized in liver fibrosis by the conversion of vitamin A storage cells into expressed myofibroblasts and plays a key role.<sup>5</sup> Excessive expression of profibrotic genes has been found in liver fibrosis, such as type I collagen  $\alpha 1$  chain (Col1 $\alpha 1$ ), type I collagen  $\alpha 2$  chain (Col1 $\alpha 2$ ),  $\alpha$ -smooth muscle actin ( $\alpha$ -SMA), fibrin Connexin 1 (Fn1), tissue inhibitor of metalloproteinase-1 (TIMP1).  $\alpha$ -SMA intensifies the contractile force of HSC by combining stress fibers and is a marker of activated HSC.<sup>6,7</sup> HSC contraction leads to an increase in liver stiffness and sinusoidal contraction, which are two critical factors that lead to liver complications, such as portal hypertension.<sup>8,9</sup> Identifying molecules that regulate activation of HSC and hepatic fibrogenesis can provide new therapeutic targets.

Leucine-rich repeats and immunoglobulin 1 (LRIG1), a negative regulator of EGFR localized at 3p14, which encodes 3 Ig-like domain trans membrane proteins and 15 leucine-rich repeats in its extracellular region, serves as a tumor suppressor and negative receptor tyrosine kinases (RTK) regulator,<sup>10-14</sup> and is down-regulated in renal cell carcinoma, glioma, advanced cervical cancer, and breast cancer.<sup>15-19</sup> However, the role of LRIG1 in liver fibrosis is unclear. Recently, several studies have shown that LRIG1 regulates the invasiveness of head and neck tumors by regulation of extracellular matrix remodeling and the EGFR-MAPK-SphK1 pathway. Down-regulation of LRIG1 enhances the EGFR-MAPK-SphK1 pathway and ECM remodeling activity.<sup>20</sup> In summary, it is speculated that LRIG1 may play important roles in liver fibrosis.

Sphingosine-1-phosphate (S1P) acts on a multi-effect lipid medium on the cell surface or through the G protein-coupled S1P receptor at the intracellular target site, and S1P can be converted from sphingosine to two kinds of sphingosine Alcohol kinase isoforms (SphK1 and SphK2).<sup>21</sup> S1P is currently considered to be an important regulator of kidney, lung, skin fibrosis and heart with potent cell chemotaxis in chemokines and inflammatory mediators.<sup>22-29</sup> Recent studies have reported that the S1P/SphK1/S1PR signaling axis is

involved in liver fibrosis and damage.<sup>30-33</sup> SphK1 inhibitors decrease angiogenesis and prevent differentiation in the liver fibrotic model of mice.<sup>32</sup> During liver injury, bone marrow mesenchymal stem cells (BMSCs) spread to myofibroblasts suggesting that targeting SphK1 may be a new therapeutic strategy for the treatment of liver fibrosis.<sup>34,35</sup> A previous paper by González-Fernández et al<sup>36</sup> showed that mice receiving CCl<sub>4</sub> and TGF- $\beta$ -treated LX2 cells, abrogated the lipid pathway by the indole, revealing the interest of targeting the sphingolipid pathway to facilitate the development of therapies for liver fibrosis. This study aims to investigate the role of LRIG1 in improving HSC activation and liver fibrosis by inhibiting the SphK1/S1P signaling pathway.

## MATERIALS AND METHODS

### Animal and Treatment Protocol

Guizhou Provincial People's Hospital provided the Male C57BL/6J mice (n=12, 20-25 g) in the study. Mice were acclimated to a controlled chamber at a temperature of 25 °C and a humidity of 55%, and a twelve to twelve hours light-dark cycle was performed at least one week before the experiment. Mice were allowed to eat food and water ad libitum. Mice (n=6) were intraperitoneal injection with 10% carbon tetrachloride (CCl<sub>4</sub>) in olive oil at 0.01 mL/g body weight every two weeks for eight weeks. Control mice received injections of olive oil (n=6). The research protocol was carried out according to the requirement of the National Institutes of Health Laboratory Animal Care and Use Guidelines and was specifically approved through the Ethics Committee of the Guizhou Provincial People's Hospital (Approval no. 1900629). Mice were anesthetized with a ketamine/xylazine cocktail and sacrificed at the end of the experiment. Serum samples were collected and stored at -80 °C for further analysis. Livers were collected for analysis twenty-four hours after the last injection of CCl<sub>4</sub>. The specific SphK1 inhibitor SKI-5c (10  $\mu$ M/Kg, Merck Millipore, Germany) was dissolved in 0.01% DMSO.

### LX-2 Culture and Treatments

Human HSCs cell line LX-2 was kindly provided by the American Type Culture Collection (ATCC, Manassas, USA). Stock cell lines were grown in a single layer in a 5% CO<sub>2</sub> humidification incubator at 37°C. The cultured medium used was DMEM (Sigma,

## LRIG1 Ameliorates Cell Activation via Inhibiting SphK/S1P Pathway

St Louis, MO, USA) supplemented with penicillin (100 U/mL), streptomycin (100 mg/mL) and 10% fetal bovine serum (FBS). The medium was replaced with fresh medium (2% FBS) after twenty-four hours. PBS+NC cells were cultured with 0.05% PBS, and TGF- $\beta$ +NC cells were cultured with 0.05% PBS and 10 ng/mL TGF- $\beta$  (R&D System, Minneapolis, MN). PBS+LRIG1 cells were transfected with LRIG1 (100 nM), and TGF- $\beta$ +LRIG1 cells were treated with TGF- $\beta$  (10 ng/mL) and transfected with LRIG1 (100 nM) using Lipofectamine 2000 reagent (Invitrogen, Groningen, the Netherlands) according to the manufacturer's instructions. Cells were cultured for 24 h.

### Transfection and siRNA Knockdown

Recombinant viruses were generated from 293 packaging cells co-transfected with the AdMax<sup>TM</sup> system (Microbix, ON, Canada) using a shuttle plasmid and a framework plasmid (pBHGlox, Thermo Scientific, Waltham, MA, USA). siRNA sequence targeting LRIG1 (5-GCTCAGAACTCAGCCGGTTCTATTT-3) were synthesized by Invitrogen. The virus stock was purified using a CsCl gradient. The vector was constructed without the transgene (Ad. V); using the same method. The titer of the recombinant adenovirus was determined by 50 % tissue culture infectious dose.

### Hematoxylin-eosin (HE) Staining

The specimens of liver tissue were fixed in 10% formaldehyde in PBS at room temperature for twenty-four hours. The specimens were then embedded in paraffin, sliced at 4-5  $\mu$ m thickness, and then stained with heme, and analyzed using light microscopy.

### Masson Staining and Sirius Red Staining

The liver tissue was made into paraffin blocks, cut into 5  $\mu$ m sections, and dried at 60°C. For Masson staining, the sections were dewaxed with xylene, rehydrated with a gradient of alcohol, and stained with Regaud hematoxylin for six minutes. Then, the sections were soaked for 3 s in 1% hydrochloric ethanol, and stained for 1 min with acidic ponceau reagent (Sigma, St Louis, MO, USA). After soaking for a few seconds in acetic acid (0.2%) and phosphomolybdic acid (1 %) for five minutes, counterstained the sections for 5 min with aniline blue reagent, soaked for a few minutes in acetic acid (0.2%), and dehydrated with xylene and ethanol. For Sirius red staining, the nuclei were stained

for 8 min with Weigert hematoxylin and the slides were washed in running tap water for 10 min. The next sample was stained for 1 h in picrosirius red and washed in two changes acidified glasses of water. The next procedure was performed by standard procedures and finally, fibrosis and collagen fibril were observed under an optical microscope (200  $\times$ ).

### Immunofluorescence Staining

Samples of liver tissue were made into buffered formalin (10%) and embedded in paraffin. The 4  $\mu$ m sections were deparaffinized and hydrated by gradient ethanol, cooked in a pressure cooker for ten minutes in 25 mM citrate buffer (pH 6.0), transferred to boiling deionized water and allowed to cool for twenty minutes. Then, tissue sections were treated with hydrogen peroxide (3%) to inactivate the activity of endogenous peroxidase. The slides were placed in a cell culture dish for cell crawling. After climbing, the cells were fixed with paraformaldehyde (4%) and then permeabilized with Triton X-100 (0.5%) for twenty minutes at room temperature, and then normal goat serum was added dropwise on the slide. After blocking for 30 min at room temperature, the anti- $\alpha$ -SMA and Coll $\alpha$ 1 (1:500, Abcam, Cambridge, UK) were added for immunological reaction, and placed in a humid box and cultured at 4°C overnight. After the primary antibody was cultured, the fluorescent secondary antibody Cy3 (1:200) was added to the wet box for 20 h at 20-37 °C, and then DAPI was added dropwise for 5 min in the dark. The specimen was stained with nuclei, then mounted, and finally, the image was collected.

### Quantitative Real-time PCR

Rapid dissection of liver tissue on ice and extracted the total RNA by the Trizol reagent (Invitrogen, Carlsbad, CA). The SuperScript RT kit from Invitrogen (Invitrogen, Carlsbad, CA) was then used to reverse-transcribed 2  $\mu$ g of total RNA from samples. ABI Prism7900 Sequence Detection System with SYBR Green PCR Master Mix (Applied Biosystems, USA) was used to analyze mRNA expression in the culture fluids and cells.

**Table 1. The sequences of mRNA primers**

ID	Forward (5' ~ 3' )	Reverse (5' ~ 3' )
$\alpha$ -SMA	CCGACCGAATGCAGAAGG	AAGGTAGACAGCGAAGCCAA
Coll1 $\alpha$ 1	GAGACTGTTCTGTTCCCTTGTAAGT	CCCCGGTGACACATCAAGAC
LRIG1	GGTGAGCCTGGCCTTATGTGAATA	CACCACCATCCTGCACCTCC
IL-1 $\beta$	CCCTGAACTCAACTGTGAAATAGCA	CCCAAGTCAAGGGCTTGAA
IL-6	ATTGTATGAACAGCGATGATGCAC	CCAGGTAGAAACGGAAGTCCAGA
TNF- $\alpha$	CCTCTTCTCATTCTGCTC	CTTCTCCTCCTTGTTGGG
GAPDH	AAGGAAATGAATGGGCAGCC	TAGGAAAAGCATCACCCGGA

Table 1 showed the primer sequences. A control containing no cDNA was assayed in parallel for each sample. Calculating targeted gene expression as described previously by the  $2^{-\Delta\Delta CT}$  method.

### Western Blotting

Total proteins from cells or tissues were immunoblotted using the monoclonal antibodies against  $\alpha$ -SMA, LRIG1, SphK1, Coll1 $\alpha$ 1, TIMP-1, Fn-1, TGF- $\beta$ 1, S1PL (all 1:800, Sigma, USA).  $\beta$ -actin (1:5000, Santa Cruz, USA) served as a loading control. Horseradish peroxidase (HRP)-labeled secondary antibody (1:1000, Santa Cruz, USA) was used and incubated for 1 h at 25 °C. The band densities were quantified by the LICOR Odyssey infrared imaging system (LICOR Bioscience, Nebraska, USA).

### ELISA Assay

TNF- $\alpha$ , IL-1 $\beta$ , and IL-6 expression levels were measured by ELISA kits according to the manufacturer's requirement (Sigma, USA). A spectrophotometer was used to read the absorbance of each well at 450 nm, and the contents of each well were calculated using a standard curve.

### Cell Viability

The conventional MTT assay was used to analyze cell viability. LX-2 cells were plated into 96-well microplates with  $2-4 \times 10^4$  cells per well. MTT solution (Sigma, USA) was then added to the medium with 0.5 mg/mL and cultured at 37°C for 4 hours. The absorbance was measured at 450 nm and the results were analyzed.

### Caspase 3 Activity Assay

Caspase-3 assay kit (Beyotime, Shanghai, China) was used to determine the relative caspase-3 activity. Briefly, LX-2 cells were treated with paraffin in 96-well plates for 90 min and passed through 80  $\mu$ L of

reaction buffer with the caspase-3 substrate (Ac-DEVD-pNA) (2 mmol/L, 10  $\mu$ L). 10  $\mu$ L of cell lysate protein was incubated in each sample, and the lysate was cultured for two hours at 37°C. Read absorbance measurements at 405 nm by a colorimetric assay kit from R&D Systems (Sigma, USA).

### Statistical Analyses

The software GraphPad 8.0 was used to analysis of the data. All data were repeated as independent experiment triple times and presented as mean $\pm$ standard deviation (SD). ANOVA analysis was conducted to compare the significance of differences among groups. The  $p < 0.05$  was regarded as significant.

## RESULTS

### LRIG1 Was Decreased in Liver Fibrosis by CCl<sub>4</sub>-induced and Activated HSC Cells

A pulmonary fibrosis mouse model was induced by CCl<sub>4</sub>, and LRIG1 expression in CCl<sub>4</sub>-induced liver fibrosis and activated HSC cells was detected. HE staining, Sirius red staining, and Masson staining results showed that fibrosis and serious injuries in liver tissue caused by CCl<sub>4</sub> were found (Figure 1A). To examine protein levels of  $\alpha$ -SMA and Coll1 $\alpha$ 1, tissue microarrays were performed by immune fluorescence staining. The results showed that the expression levels of  $\alpha$ -SMA and Coll1 $\alpha$ 1 were significantly increased in the liver tissue of CCl<sub>4</sub>-induced mice (Figure 1B). Also, the expression of genes related to fibrogenesis was analyzed using western blot and quantitative real-time PCR. We found augmented mRNA expression of  $\alpha$ -SMA and Coll1 $\alpha$ 1 in CCl<sub>4</sub>-treated mice ( $p < 0.001$ ), and the similar results were observed in  $\alpha$ -SMA and Coll1 $\alpha$ 1 protein expression (Figure 1C and 1D,  $p < 0.01$ ,  $p < 0.001$ ). LRIG1 mRNA levels in LX-2 cell lines and CCl<sub>4</sub>-induced mice were then analyzed by qRT-PCR.

## LRIG1 Ameliorates Cell Activation via Inhibiting SphK/S1P Pathway

Figure 1E showed that LRIG1 was markedly downregulated.

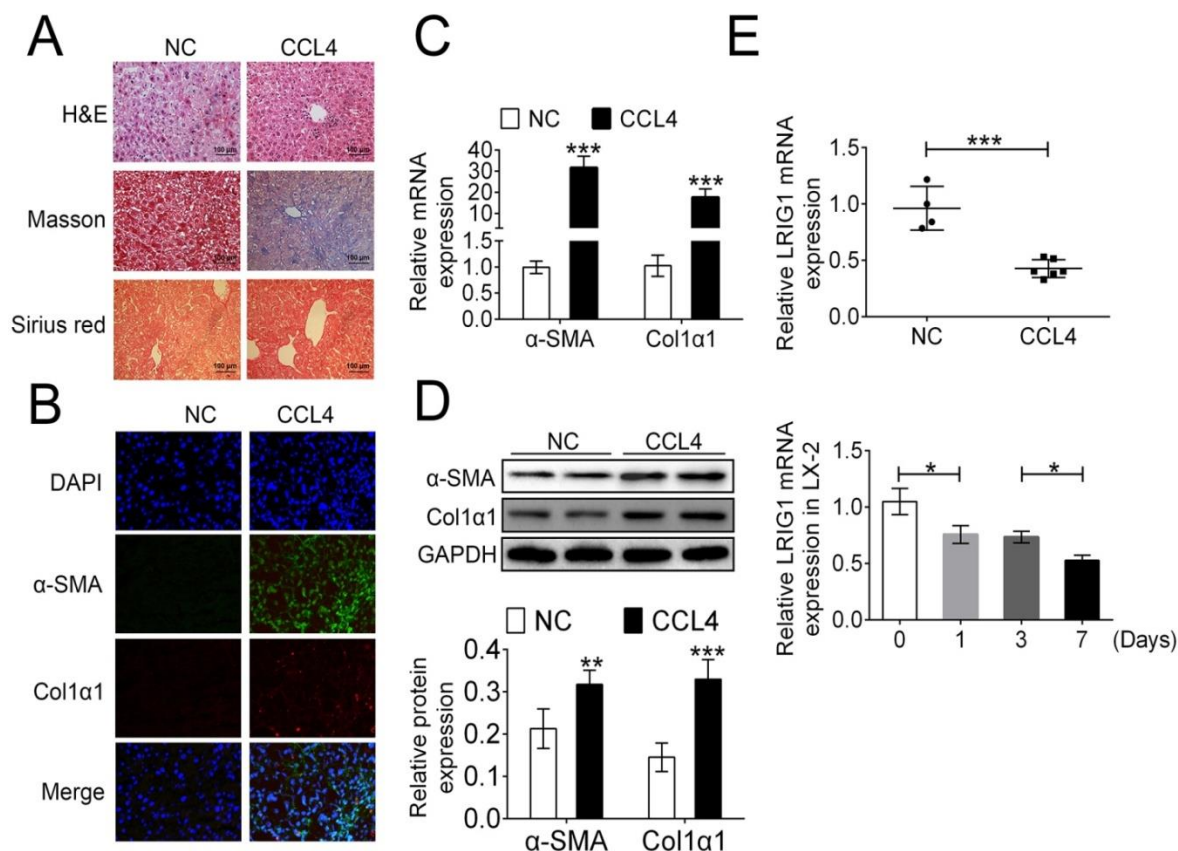


**Figure 1.** leucine-rich repeats and immunoglobulin 1 (LRIG1) expression in carbon tetrachloride (CCl<sub>4</sub>)-induced liver fibrosis and activated hepatic stellate cell (HSC) cells. Figure 1A. H & E staining, Masson staining, Sirius red staining for liver tissue morphology, scale bar = 100  $\mu$ m. Figure 1B. Immunofluorescence detection of  $\alpha$ -smooth muscle actin ( $\alpha$ -SMA) and type I collagen  $\alpha$ 1 chain (Col1 $\alpha$ 1). Figure 1C and Figure 1D. qRT-PCR and western blot detection of  $\alpha$ -SMA and Col1 $\alpha$ 1 expression levels, respectively, \*\* $p$  < 0.01, \*\*\* $p$  < 0.001 vs. NC group. (E) qRT-PCR detection of LRIG1 expression level in LX-2 cells, \* $p$  < 0.05 vs. 0 Day or 3 Days

### Overexpression of LRIG1 Attenuated Liver Fibrosis and SphK1/S1P Pathway Activation in Mice Induced by CCl<sub>4</sub>

From the HE staining, Masson staining, and Sirius red staining results, there was no significant change in Oil group, while serious injury and fibrosis were observed in Ad. V of the CCl<sub>4</sub>group, which were alleviated by overexpression of LRIG1 (Figure 2A). Results of immune fluorescence staining showed that the several fibrosis-related protein expression levels, such as Col1 $\alpha$ 1 and  $\alpha$ -SMA were increased after CCl<sub>4</sub> employment in liver tissues as compared to the Oil group. These proteins levels were down-regulated after

overexpression of LRIG1 by transfection (Figure 2B). Due to the key effect of S1PL in fibrosis, the S1PL content was evaluated by Western blotting. The results suggested that the S1PL content in the liver tissue of the CCl<sub>4</sub>group was increased after overexpression of LRIG1 (Figure 2C). Moreover, the LRIG1 expression level was increased in Ad. V LRIG1 of Oil or CCl<sub>4</sub>group, respectively (Figure 2C). However, SphK1, a kinase necessary for activating S1PL, and few fibrosis-related proteins, Col1 $\alpha$ 1,  $\alpha$ -SMA, TIMP-1, Fn-1, TGF- $\beta$ 1 were decreased after overexpression of LRIG1 (Figure 2C). Furthermore, the qRT-PCR and ELISA results showed that the inflammatory factors,

TNF- $\alpha$ , IL-1 $\beta$ , and IL-6 were down-regulated in Ad. V of CCl<sub>4</sub> group after overexpression of LRIG1 (Figure 2D and 2E).

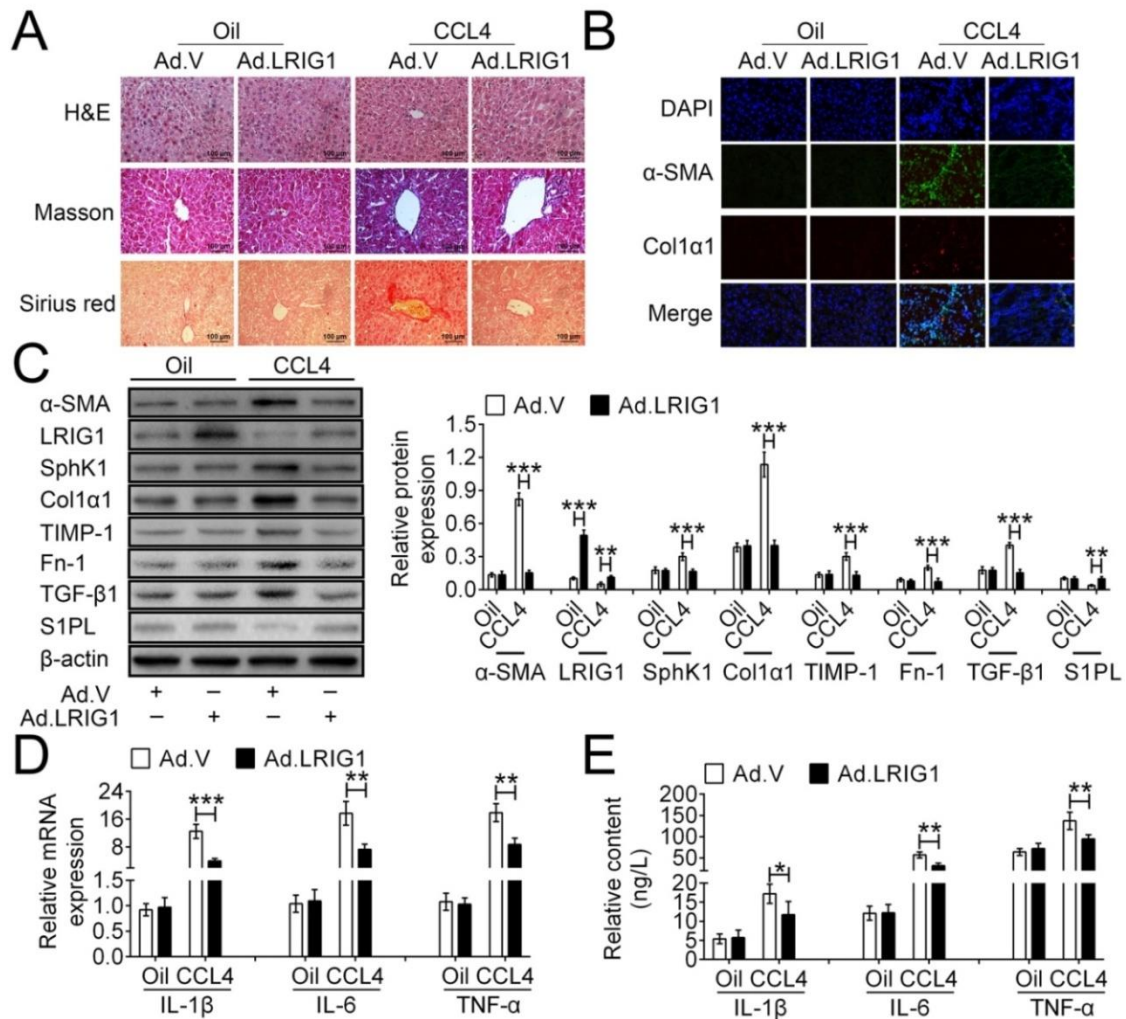


**Figure 2.** Effect of leucine-rich repeats and immunoglobulin 1 (LRIG1) overexpression on liver fibrosis and sphingosine kinase 1 (SphK1)/Sphingosine-1-Phosphate (S1P) pathway activation in mice induced by carbon tetrachloride (CCl<sub>4</sub>). Figure 2A. H & E staining, Masson staining, Sirius red staining for liver tissue morphology, scale bar = 100  $\mu$ m. Figure 2B. Immunofluorescence detection of  $\alpha$ -smooth muscle actin ( $\alpha$ -SMA) and type I collagen  $\alpha$ 1 chain (Col1 $\alpha$ 1). Figure 2C. Western blot analysis of  $\alpha$ -SMA, LRIG1, SphK1, Col1 $\alpha$ 1, TIMP-1, Fn-1, transforming growth factor-beta 1 (TGF- $\beta$ 1), S1PL expression, \*\* $p$ < 0.01, \*\*\* $p$ <0.001 vs. Ad. V group. Figure 2D) &Figure 2E. qRT-PCR and ELISA for TNF- $\alpha$ , IL-6, and IL-1 $\beta$  content, \*\*\* $p$ < 0.001 vs. Ad. V of Oil group, \* $p$ < 0.05, \*\* $p$ < 0.01, \*\*\* $p$ < 0.001 vs. Ad. V of CCl<sub>4</sub> group

### LRIG1 Attenuated HSCs Fibrosis Induced by TGF- $\beta$ and SphK1/S1P Pathway Activation

LX-2 cells were used as an in vitro model to examine the potential effects of fibroblasts in liver fibrosis. The results of MTT assays showed that the same trend in the cell viability of PBS + NC and PBS + LRIG1 group. After TGF- $\beta$  induction, the cell viability was markedly decreased in the TGF- $\beta$  + NC group,

however, LRIG1 significantly promoted the proliferation rate of LX-2 cells in the TGF- $\beta$ +LRIG1 group (Figure 3A,  $p$ <0.05). The caspase 3 activity assay revealed that the apoptosis of PBS+NC and PBS+LRIG1 group had the same trend and the apoptosis of LX-2 cells was significantly increased after TGF- $\beta$  treatment, while the apoptosis was restored by LRIG1 treatment (Figure 3B,  $p$ <0.05). The western

## LRIG1 Ameliorates Cell Activation via Inhibiting SphK/S1P Pathway

blotting results revealed that the expression of  $\alpha$ -SMA, SphK1, Col1 $\alpha$ 1, TIMP-1, Fn-1, TGF- $\beta$ 1, and S1PL were in the same trend, whereas the expression of LRIG1 was markedly higher than that in PBS + NC group ( $p < 0.01$ ). However, the S1PL and LRIG1 contents in LX-2 cells were decreased and  $\alpha$ -SMA, SphK1, Col1 $\alpha$ 1, TIMP-1, Fn-1, TGF- $\beta$ 1 contents were increased after TGF- $\beta$  treatment, while there were opposite results after LRIG1 transfection (Figure 3C).

### SphK1 Inhibitor Reversed the Effect of shLRIG1 on Liver Fibrosis of Mice Induced by CCl<sub>4</sub>

To verify whether the SphK1/S1P pathway affects the role of LRIG1 on fibrosis, SphK1 inhibitor was used in the presence of shLRIG1 treatments in CCl<sub>4</sub>-induced mice. As shown in Figure 4A, the HE, Masson,

and Sirius red staining results showed the serious inflamed area, collagen area, and fibrous area in Ad. LRIG1-siRNA group, whereas these effects were alleviated by the SphK1 inhibitor. Fibrosis-related protein, S1PL and LRIG1 contents were decreased after shLRIG1 application and  $\alpha$ -SMA, SphK1, Col1 $\alpha$ 1, TIMP-1, Fn-1, TGF- $\beta$ 1 contents were increased by shLRIG1 treatment in CCl<sub>4</sub>-induced mice (all  $p < 0.05$ ), while there were opposite results in these protein contents after SphK1 inhibitor treatment in CCl<sub>4</sub>-induced mice (Figure 4B, all  $p < 0.001$ ). Then, the inflammatory factors, TNF- $\alpha$ , IL-1 $\beta$ , and IL-6, expression levels were evaluated in CCl<sub>4</sub>-induced mice by ELISA and qRT-PCR. The results suggested that the TNF- $\alpha$ , IL-6, and IL-1 $\beta$  expression level was promoted by shLRIG1. However, the promotion was attenuated by SphK1 inhibitor (Figure 4C and 4D).

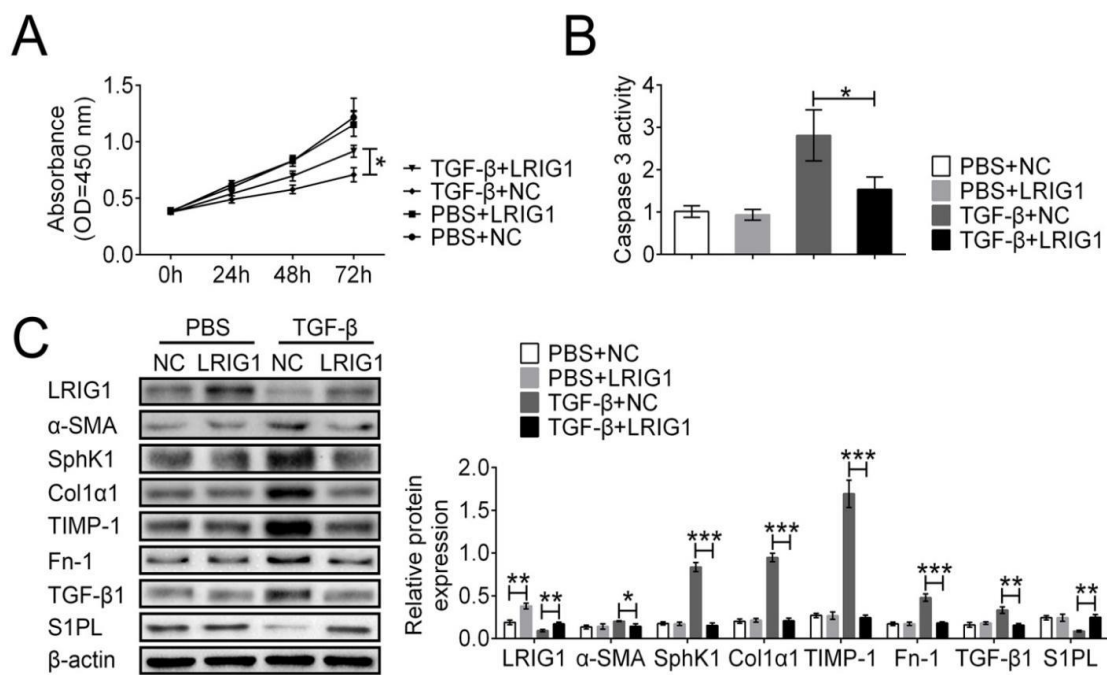


**Figure 3.** Effect of leucine-rich repeats and immunoglobulin 1 (LRIG1) on the hepatic stellate cells (HSCs) fibrosis induced by transforming growth factor-beta 1 (TGF- $\beta$ ) and sphingosine kinase 1 (SphK1)/ Sphingosine-1-Phosphate (S1P) pathway activation. Figure 3A. MTT assay for cell proliferation,  $*p < 0.05$  vs. TGF- $\beta$  + NC group. Figure 3B. Caspase3 activity assay detection of apoptosis,  $*p < 0.05$  vs. TGF- $\beta$  + NC group. Figure 3C. Western blot analysis of  $\alpha$ -smooth muscle actin ( $\alpha$ -SMA), LRIG1, SphK1, type I collagen  $\alpha$ 1 chain (Col1 $\alpha$ 1), TIMP-1, Fn-1, TGF- $\beta$ 1, S1PL expression,  $**p < 0.01$  vs. PBS + NC group,  $*p < 0.05$ ,  $**p < 0.01$ ,  $***p < 0.001$  vs. TGF- $\beta$  + NC group

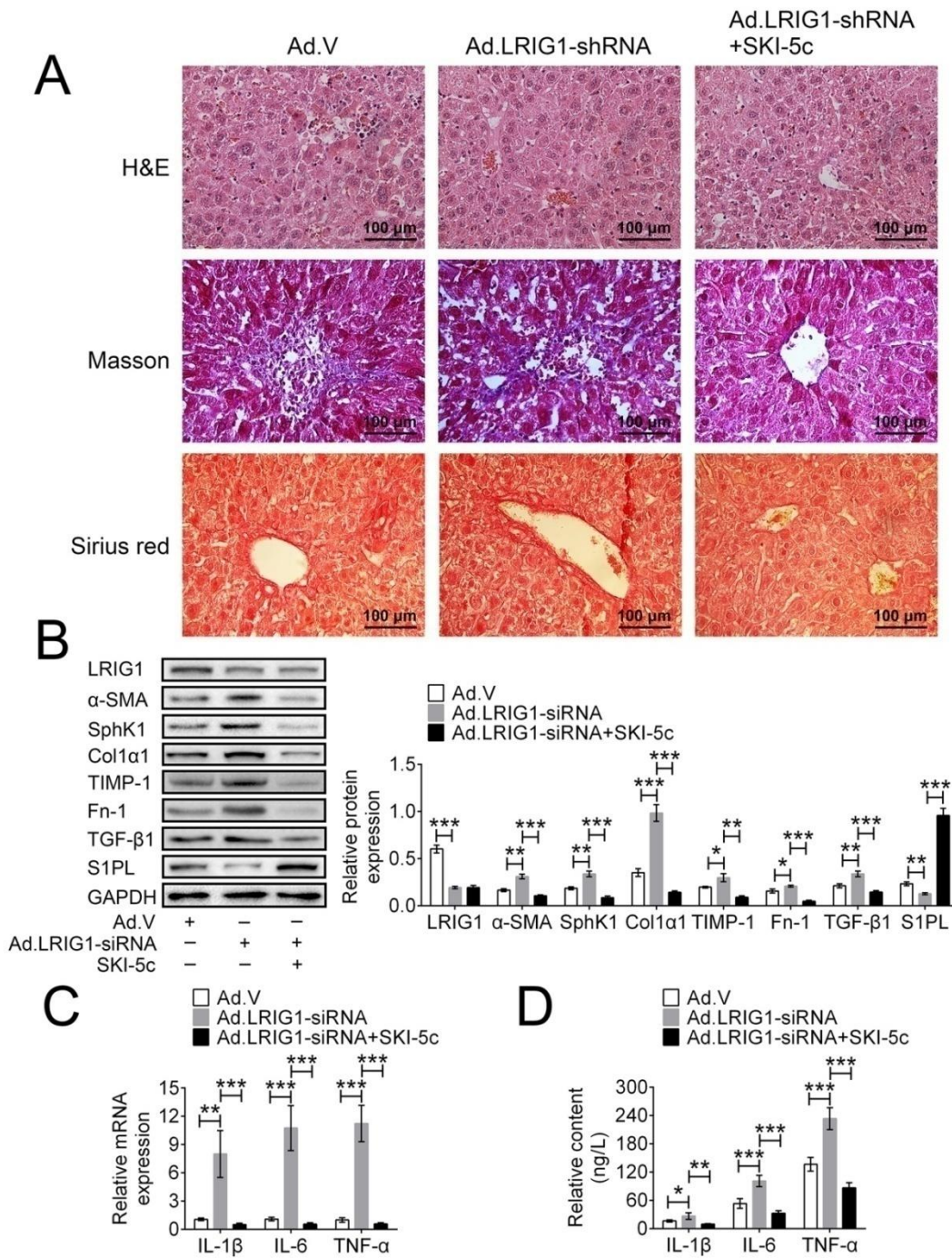


**Figure 4.** sphingosine kinase 1 (SphK1) inhibitor reversed the effect of shLRIG1 on liver fibrosis of mice induced by carbon tetrachloride (CCl<sub>4</sub>). **Figure 4A.** H & E staining, Masson staining, Sirius red staining for liver tissue morphology, scale bar = 100  $\mu$ m. **Figure 4B.** Western blot analysis of  $\alpha$ -smooth muscle actin ( $\alpha$ -SMA), leucine-rich repeats and immunoglobulin 1 (LRIG1), SphK1, type I collagen  $\alpha$ 1 chain (Col1 $\alpha$ 1), TIMP-1, Fn-1, transforming growth factor-beta 1 (TGF- $\beta$ 1), S1PL expression, \* $p$ <0.05, \*\* $p$ < 0.01, \*\*\* $p$ <0.001 vs. Ad. V group, \*\* $p$ <0.01, \*\*\* $p$ <0.001 vs. Ad. LRIG1-siRNA group. **Figure 4C&Figure 4D.** qRT-PCR and ELISA for TNF- $\alpha$ , IL-6 and IL-1 $\beta$  content, \* $p$ < 0.05, \*\* $p$ < 0.01, \*\*\* $p$ < 0.001 vs. Ad. V group, \*\* $p$ <0.01, \*\*\* $p$ <0.001 vs. Ad. LRIG1-siRNA group



## DISCUSSION

The current findings provided the first evidence that leucine-rich repeats and immunoglobulin 1 (LRIG1) ameliorated liver fibrosis and hepatic stellate cell (HSC) activation by inhibiting SphK1/S1P pathway. Our results also demonstrated that overexpression of LRIG1 attenuated liver fibrosis and SphK1/S1P pathway activation in mice induced by CCl<sub>4</sub>. LRIG1 attenuated HSCs fibrosis induced by TGF- $\beta$  and SphK1/S1P pathway activation. Also, the SphK1 inhibitor was used in the presence of shLRIG1 treatments in CCl<sub>4</sub>-induced mice. SphK1 inhibitor reversed the effect of shLRIG1 on CCl<sub>4</sub>-induced liver fibrosis in mice.

As a component of the plasma membrane, sphingosine is the backbone of most sphingolipids. By binding to various functional groups, sphingosine is derived from varieties of biologically active molecules, including sphingomyelin, S1P, lysophosphatidic acid, and ceramide.<sup>37</sup> S1P is synthesized by SphK1 or SphK2 and is degraded by S1P phosphatase, S1PL or lipid phosphate phosphatase.<sup>21</sup> S1P is now recognized as a pivotal regulator of fibrosis diseases and the relevance of SphK1/S1P signaling has been shown in different animal models of liver fibrosis, human fibrotic samples, and HSCs.<sup>38,39</sup> Previous researches have also found that LRIG1 may have a regulatory effect on fibrotic pathogenesis and have protective effects against fibrosis in several tissues and organs, including the liver.<sup>40</sup> The results here obtained in a CCl<sub>4</sub>-induced model of liver fibrogenesis suggest that LRIG1 was decreased in liver fibrosis *in vivo* and *in vitro*.

LRIG1 which is a negative regulator of EGFR and localized at 3p14 has been proposed as a tumor suppressor gene, which encodes 3 Ig-like domain transmembrane proteins and 15 leucine-rich repeats in its extracellular region.<sup>41,42</sup> In head and neck tumors, LRIG1 (chromosome 3p) and EGFR amplification deletion are frequently observed pathogenic events in tumor tissues.<sup>42-44</sup> Clinically, both LRIG1 downregulation and EGFR overexpression are related to a poor clinical result. Biologically, LRIG1 acts as a negative regulator to inhibit ECM remodeling by positive-feedback inhibitory regulation and the EGFR-MAPK-SPHK1 pathway.<sup>45</sup> In the present study, the serious injury and fibrosis of the CCl<sub>4</sub> group were alleviated by the overexpression of LRIG1. Results of immunoblotting showed that several fibrosis-related

proteins expression levels, including  $\alpha$ -SMA and Coll $\alpha$ 1 in CCl<sub>4</sub>-induced mice, were decreased after overexpression of LRIG1. The results of western blot suggested that the content of S1PL in the liver tissue of the CCl<sub>4</sub> group was increased after overexpression of LRIG1. SphK1, a kinase necessary for activating S1PL, and few fibrosis-related proteins, Coll $\alpha$ 1,  $\alpha$ -SMA, TIMP-1, Fn-1, TGF- $\beta$ 1 were decreased after overexpression of LRIG1. Moreover, the results of qRT-PCR and ELISA showed that the inflammatory factors, TNF- $\alpha$ , IL-1 $\beta$ , and IL-6, were down-regulated in the CCl<sub>4</sub> group after overexpression of LRIG1.

Earlier studies suggested that HSCs are fully differentiated myofibroblasts with a low sensitivity towards TGF- $\beta$ .<sup>46</sup> We found an appropriate response of HSC to TGF- $\beta$  that confirms other recent research with an adequate experimental setting involving early passages of cells.<sup>47</sup> LRIG1 treatment reversal of activated LX-2 cells was confirmed by a reduced expression of  $\alpha$ -SMA, TGF- $\beta$  and Col I, which was similar to results by other researches when LX-2 cells are treated the energy blocker 3-bromopyruvate.<sup>48</sup> The present study showed that LRIG1 promoted the proliferation rate of LX-2 cells as early as 72 h after TGF- $\beta$ -induced. The caspase3 activity assay revealed that the apoptosis of LX-2 cells treated with TGF- $\beta$  was decreased after LRIG1 transfection. The western blot data revealed that the S1PL and LRIG1 contents in LX-2 cells were increased and SphK1,  $\alpha$ -SMA, Coll $\alpha$ 1, TIMP-1, Fn-1, TGF- $\beta$ 1 contents were decreased after TGF- $\beta$  treatment, while there were opposite effects by overexpression of LRIG1.

Different studies show that SphK1 is a downstream mediator of TGF- $\beta$  signaling.<sup>49</sup> It is also known that decrease of SphK1 expression by siRNA blocks TGF- $\beta$ -mediated upregulation of TIMP-1, a protein that plays a critical role in matrix modeling and degradation.<sup>50,51</sup> We have recently reported that in melatonin-treated mice the expression of TIMP-1 was decreased,<sup>11</sup> which could thus be a consequence of the inhibition in the SphK1/S1P axis and explains, at least in part, the abrogation of TGF- $\beta$  mitogenic effects. Our data are consistent with previous studies which showed that, after the administration of SphK1 inhibitors, the HE staining, Masson staining, and Sirius red staining results showed that serious injury and fibrosis were alleviated. Fibrosis-related protein, S1PL, and LRIG1 levels were decreased and  $\alpha$ -SMA, SphK1, Coll $\alpha$ 1, TIMP-1, Fn-1, TGF- $\beta$ 1 expression were decreased by

SphK1 inhibitor in CCl<sub>4</sub>-induced mice. Therefore, the inflammatory factors, TNF- $\alpha$ , IL-6, and IL-1 $\beta$  expression levels were downregulated by SphK1 inhibitor.

In conclusion, the results of the present study indicated that LRIG1 ameliorated liver fibrosis in mice induced by CCl<sub>4</sub> and fibrosis in LX-2 cells induced by TGF- $\beta$  via suppressing SphK1/S1P pathway, which may be explored as an important therapeutic target for treating liver fibrosis.

### CONFLICT OF INTEREST

The authors declare that they have no competing interests, and all authors should confirm their accuracy.

### ACKNOWLEDGEMENTS

This work was supported by the Science and Technology Fund Project of Guizhou Health and Family Planning Commission. (Grant No. gzwjkj-2018-1-035), and the Science and Technology Fund Project of Guizhou Health and Family Planning Commission (Grant No. gzwjkj-2018-1-075).

### REFERENCES

- Wallace K, Burt AD, Wright MC. Liver fibrosis. *Biochem J*. 2008;411(1):1-18.
- Hernandez-Gea V, Friedman SL. Pathogenesis of Liver Fibrosis. *Annu Rev Pathol* 2011;6(1):425-56.
- Nyström H, Naredi P, Hafström L, Sund M. Type IV collagen as a tumour marker for colorectal liver metastases. *Eur J Surg Oncol*. 2011;37(7):611-7.
- Zhang DY, Friedman SL. Fibrosis-dependent mechanisms of hepatocarcinogenesis. *Hepatology*. 2012;56(2):769-75.
- Beuge MMV, Prakash J, Lacombe M, Post E, Reker-Smit C, Beljaars L, et al. Increased Liver Uptake and Reduced Hepatic Stellate Cell Activation with a Cell-Specific Conjugate of the Rho-kinase Inhibitor Y27632. *Pharm Res*. 2011;28(8):2045-54.
- Chaponnier C, Goethals M, Janmey PA, Gabbiani F, Gabbiani G, Vandekerckhove J. The specific NH<sub>2</sub>-terminal sequence Ac-EEED of alpha-smooth muscle actin plays a role in polymerization in vitro and in vivo. *J Cell Biol*. 1995;130(4):887-95.
- Hinz B, Celetta G, Tomasek JJ, Gabbiani G, Chaponnier C. Alpha-Smooth Muscle Actin Expression Upregulates Fibroblast Contractile Activity. *Mol Biol Cell*. 2001;12(9):2730-41.
- Jr RKS, Jr HFY. Stellate Cell Contraction: Role, Regulation, and Potential Therapeutic Target. *Clin Liver Dis*. 2008;12(4):791-803.
- Pinzani M, Rosselli M, Zuckermann M. Liver cirrhosis. *Lancet*. 2008;371(9615):838-51.
- Laederich MB, Melanie FD, Lily Y, Ellen I, Xiuli W, Carraway KL, et al. The leucine-rich repeat protein LRIG1 is a negative regulator of ErbB family receptor tyrosine kinases. *J Biol Chem*. 2004;279(45):47050-6.
- Gal G, Chanan R, Menachem K, Ido A, Ami C, Jonas N, et al. LRIG1 restricts growth factor signaling by enhancing receptor ubiquitylation and degradation. *Embo Journal*. 2014;23(16):3270-81.
- Zhou L, Li X, Zhou F, Jin ZA, Chen D, Wang P, et al. Down - regulation of LRIG1 by microRNA - 20a modulates gastric cancer multidrug resistance. *Cancer Science*. 2018;109(4):1044-54.
- Yang NY, Zhou Y, Zhao HY, Liu XY, Sun Z, Shang JJ. Increased interleukin 1 $\alpha$  and interleukin 1 $\beta$  expression is involved in the progression of periapical lesions in primary teeth. *Bmc Oral Health*. 2018;18(1):124-30.
- Lindquist D, Alsina FC, Herdenberg C, Larsson C, Höppener J, Wang N, et al. LRIG1 negatively regulates RET mutants and is downregulated in thyroid cancer. *International Journal of Oncology*. 2018;52(4):1189-97.
- Thomasson M, Hedman H, Guo D, Ljungberg B, Henriksson R. LRIG1 and epidermal growth factor receptor in renal cell carcinoma: a quantitative RT-PCR and immunohistochemical analysis. *Br J Cancer*. 2003;89(7):1285-9.
- Miller JK, Shattuck DL, Ingalla EQ, Lily Y, Borowsky AD, Young LJT, et al. Suppression of the negative regulator LRIG1 contributes to ErbB2 overexpression in breast cancer. *Cancer Res*. 2008;68(20):8286-94.
- Stutz M, Shattuck DM, Sweeney C. LRIG1 negatively regulates the oncogenic EGF receptor mutant EGFRvIII. *Oncogene*. 2008;27(43):5741-52.
- Ljuslinder I, Golovleva I, Henriksson R, Grankvist K, Malmer B, Hedman H. Co-incident increase in gene copy number of ERBB2 and LRIG1 in breast cancer. *Breast Cancer Res*. 2009;11(3):403-5.
- Lindström AK, Ekman K, Stendahl U, Tot T, Henriksson R, Hedman H, et al. LRIG1 and squamous epithelial uterine cervical cancer: correlation to prognosis, other tumor markers, sex steroid hormones, and smoking. *Int J Gynecol Cancer*. 2010;18(2):312-7.
- J J-C S, C-C L, C-H H, C-I L, M-T L, S-C L, et al.

## LRIG1 Ameliorates Cell Activation via Inhibiting SphK/S1P Pathway

- LRIG1 modulates aggressiveness of head and neck cancers by regulating EGFR-MAPK-SPHK1 signaling and extracellular matrix remodeling. *Oncogene*. 2014;33(11):1375-84.
21. Sarah S, Sheldon M. Sphingosine-1-phosphate: an enigmatic signalling lipid. *Nat Rev Mol Cell Biol*. 2003;4(5):397-407.
  22. Long DA, Price KL. Sphingosine kinase-1: a potential mediator of renal fibrosis. *Kidney Int*. 2009;76(8):815-7.
  23. Nicole GL, Swaney JS, Moreno KM, Sabbadini RA. Sphingosine-1-phosphate and sphingosine kinase are critical for transforming growth factor-beta-stimulated collagen production by cardiac fibroblasts. *Cardiovasc Res*. 2009;82(2):303-12.
  24. Long Shuang H, Evgeny B, Biji M, Panfeng F, Gorshkova IA, Donghong H, et al. Targeting sphingosine kinase 1 attenuates bleomycin-induced pulmonary fibrosis. *FASEB J*. 2013;27(4):1749-60.
  25. Schwalm S, Pfeilschifter J, Huwiler A. Sphingosine-1-phosphate: a Janus-faced mediator of fibrotic diseases. *Biochim Biophys Acta*. 2013;1831(1):239-50.
  26. Shizhong B, Yoshihide A, Andreea B, Kristin H, Faye H, Maria T. Dihydrosphingosine 1-phosphate has a potent antifibrotic effect in scleroderma fibroblasts via normalization of phosphatase and tensin homolog levels. *Arthritis Rheum*. 2014;62(7):2117-26.
  27. Gonz lez-Fern ndez B, S nchez DI, Crespo I, San-Miguel B,  lvarez M, Tu n MJ, et al. Inhibition of the SphK1/S1P signaling pathway by melatonin in mice with liver fibrosis and human hepatic stellate cells. *Biofactors*. 2016;43(2):272-82.
  28. Rohrbach T, Maceyka M, Spiegel S. Sphingosine kinase and sphingosine-1-phosphate in liver pathobiology. *Crit Rev Biochem Mol Biol*. 2017;52(5):543-53.
  29. Wang E, He X, Zeng M. The Role of S1P and the Related Signaling Pathway in the Development of Tissue Fibrosis. *Front Pharmacol*. 2019;9:1504-18.
  30. Changyong L, Xiangming J, Lin Y, Xihong L, Shi Y, Liying L. Involvement of sphingosine 1-phosphate (S1P)/S1P3 signaling in cholestasis-induced liver fibrosis. *Am J Pathol*. 2009;175(4):1464-72.
  31. Li C, Zheng S, You H, Liu X, Lin M, Yang L, et al. Sphingosine 1-phosphate (S1P)/S1P receptors are involved in human liver fibrosis by action on hepatic myofibroblasts motility. *J Hepatol*. 2011;54(6):1205-13.
  32. Yang L, Yue S, Yang L, Liu X, Han Z, Zhang Y, et al. Sphingosine kinase/sphingosine 1-phosphate (S1P)/S1P receptor axis is involved in liver fibrosis-associated angiogenesis. *J Hepatol*. 2013;59(1):114-23.
  33. Xiu L, Chang N, Yang L, Liu X, Yang L, Ge J, et al. Intracellular sphingosine 1-phosphate contributes to collagen expression of hepatic myofibroblasts in human liver fibrosis independent of its receptors. *Am J Pathol*. 2015;185(2):387-98.
  34. Yang L, Chang N, Liu X, Han Z, Zhu T, Li C, et al. Bone Marrow-Derived Mesenchymal Stem Cells Differentiate to Hepatic Myofibroblasts by Transforming Growth Factor- $\beta$ 1 via Sphingosine Kinase/Sphingosine 1-Phosphate (S1P)/S1P Receptor Axis. *Am J Pathol*. 2012;181(1):85-97.
  35. Lan T, Li C, Yang G, Sun Y, Zhuang L, Ou Y, et al. Sphingosine kinase 1 promotes liver fibrosis by preventing miR-19b-3p-mediated inhibition of CCR2. *Hepatology*. 2018;68(3):1070-86.
  36. Gonz lez-Fern ndez B, S nchez DI, Crespo I, San-Miguel B,  lvarez M, Tu n MJ, et al. Inhibition of the SphK1/S1P signaling pathway by melatonin in mice with liver fibrosis and human hepatic stellate cells. *Biofactors*. 2016;43(2):272-82.
  37. Yang Y, Uhlig S. The role of sphingolipids in respiratory disease. *Ther Adv Respir Dis*. 2011;5(5):325-44.
  38. Huang LS, Berdyshev EV, Tran JT, Xie L, Chen J, Ebenezer DL, et al. Sphingosine-1-phosphate lyase is an endogenous suppressor of pulmonary fibrosis: role of S1P signalling and autophagy. *Thorax*. 2015;70(12):1138-48.
  39. Takuwa Y, Ikeda H, Okamoto Y, Takuwa N, Yoshioka K. Sphingosine-1-phosphate as a mediator involved in development of fibrotic diseases. *Biochim Biophys Acta*. 2013;1831(1):185-92.
  40. Succony L, Gowers K, Hynds RE, Thakrar R, Giangreco A, Davies D, et al. S9 The role of LRIG1-dependent EGFR signalling in airway homeostasis and squamous cell lung cancer development. *Thorax*. 2016;71(3):3-8.
  41. H H, Jonas N, Dongsheng G, Roger H. Is LRIG1 a tumour suppressor gene at chromosome 3p14.3 *Acta Oncol*. 2002;41(4):352-4.
  42. Sheu JJ, Lee Chko JY. Chromosome 3p12.3-p14.2 and 3q26.2-q26.32 are genomic markers for prognosis of advanced nasopharyngeal carcinoma. *Cancer Epidemiol Biomarkers Prev*. 2009;18(10):2709-16.
  43. Yuesheng J, Charlotte J, Mei L, Sai-Wah T, Jingke Z, Johan W, et al. Karyotypic evolution and tumor progression in head and neck squamous cell carcinomas. *Cancer Genet Cytogenet*. 2005;156(1):1-7.
  44. Abhold EL, Kiang A, Rahimy E, Kuo SZ, Wangrodriguez J, Lopez JP, et al. EGFR Kinase Promotes Acquisition of Stem Cell-Like Properties: A Potential Therapeutic Target in Head and Neck Squamous Cell Carcinoma Stem Cells. *Plos One*. 2012;7(2):32459-67.
  45. Burtneß B. The role of cetuximab in the treatment of

- squamous cell cancer of the head and neck. *Expert Opin Biol Ther.* 2005;5(8):1085-93.
46. Pyne NJ, Susan P. Sphingosine 1-phosphate and cancer. *Nat Rev Cancer.* 2010;10(7):489-503.
47. Selvam SP, Ogretmen B. Sphingosine kinase/sphingosine 1-phosphate signaling in cancer therapeutics and drug resistance. *Handb Exp Pharmacol.* 2013;216(216):3-27.
48. Susan P, Robert B, Pyne NJ. Sphingosine kinase inhibitors and cancer: seeking the golden sword of Hercules. *Cancer Res.* 2011;71(21):6576-82.
49. Fukuda, Yu, Kihara, Akio, Igarashi, Yasuyuki. Distribution of sphingosine kinase activity in mouse tissues: contribution of SPHK1. *Biochem Biophys Res Commun.* 2003;309(1):155-60.
50. Powell A, Wang Y, Li Y, Poulin E, Means A, Washington M, et al. The Pan-ErbB Negative Regulator *Lrig1* Is an Intestinal Stem Cell Marker that Functions as a Tumor Suppressor. *Cell.* 2012;149(1):146-58.
51. Chen, Wu, Fu, Feng. Expression of MMP-2 and TIMP-1 in cerebrospinal fluid and the correlation with dynamic changes of serum PCT in neonatal purulent meningitis. *Exp Ther Med.* 2018;15(2):1285-8.